Iron silicide formation at different layers of (Fe/Si)3 multilayered structures determined by conversion electron Mössbauer spectroscopy

L. Badía-Romano, J. Rubín, C. Magén, D. E. Bürgler, and J. Bartolomé

Citation: Journal of Applied Physics **116**, 023907 (2014); doi: 10.1063/1.4887522
View online: http://dx.doi.org/10.1063/1.4887522
View Table of Contents: http://scitation.aip.org/content/aip/journal/jap/116/2?ver=pdfcov
Published by the AIP Publishing

Iron silicide formation at different layers of $(Fe/Si)_3$ multilayered structures determined by conversion electron Mössbauer spectroscopy

L. Badía-Romano,[1,a)] J. Rubín,[2] C. Magén,[3] D. E. Bürgler,[4] and J. Bartolomé[1]
[1]*Departamento de Física de la Materia Condensada, Instituto de Ciencia de Materiales de Aragón, CSIC-Universidad de Zaragoza, E-50009 Zaragoza, Spain*
[2]*Departamento de Ciencia y Tecnología de Materiales y Fluidos, Instituto de Ciencia de Materiales de Aragón, CSIC-Universidad de Zaragoza, E-50018 Zaragoza, Spain*
[3]*Laboratorio de Microscopías Avanzadas (LMA), Instituto de Nanociencia de Aragón (INA), Universidad de Zaragoza, E-50018 Zaragoza, Spain*
[4]*Peter Grünberg Institut (PGI-6), Forschungszentrum Jülich GmbH, D-52425 Jülich, Germany*

(Received 3 April 2014; accepted 26 June 2014; published online 11 July 2014)

The morphology and the quantitative composition of the Fe-Si interface layer forming at each Fe layer of a $(Fe/Si)_3$ multilayer have been determined by means of conversion electron Mössbauer spectroscopy (CEMS) and high-resolution transmission electron microscopy (HRTEM). For the CEMS measurements, each layer was selected by depositing the Mössbauer active ^{57}Fe isotope with 95% enrichment. Samples with Fe layers of nominal thickness $d_{Fe} = 2.6$ nm and Si spacers of $d_{Si} = 1.5$ nm were prepared by thermal evaporation onto a GaAs(001) substrate with an intermediate Ag(001) buffer layer. HRTEM images showed that Si layers grow amorphous and the epitaxial growth of the Fe is good only for the first deposited layer. The CEMS spectra show that at all Fe/Si and Si/Fe interfaces a paramagnetic c-$Fe_{1-x}Si$ phase is formed, which contains 16% of the nominal Fe deposited in the Fe layer. The bottom Fe layer, which is in contact with the Ag buffer, also contains α-Fe and an $Fe_{1-x}Si_x$ alloy that cannot be attributed to a single phase. In contrast, the other two layers only comprise an $Fe_{1-x}Si_x$ alloy with a Si concentration of ≃0.15, but no α-Fe.
 [http://dx.doi.org/10.1063/1.4887522]

I. INTRODUCTION

In multilayers, atomic diffusion at the interfaces plays a paramount role in controlling their physical properties and therefore their potential applications. While atomic diffusion in bulk solids has been extensively studied and is quite well understood, a reasonable understanding of the interfacial diffusion in multilayers is yet desirable. Several factors such as a steep concentration gradient at the interfaces, interfacial stress, and disorder may significantly modify the diffusion in multilayers.

Especially, in ferromagnetic metal/semiconductor multilayers, as in the $(Fe/Si)_n$ multilayered structures, the Fe and Si atomic interdiffusion and subsequent reaction give rise to non-abrupt interfaces formed by one or several iron silicide phases. The formation of such new compounds can affect the physical properties of the multilayers in a positive or negative way.[1,2] For example, the presence of non-magnetic silicides decreases the current spin polarization in the silicon spacer layer and modifies the interlayer exchange coupling (IEC) mechanism. It is, therefore, of utmost importance to assess the interlayer composition.

The Fe/Si system is complex and includes a number of stable and metastable compounds produced during the layer growth process. Gomoyunova *et al.*[3] reported experimental results which support the existence of three stages in the Fe deposition on Si(100) at room temperature (RT):[4,5] formation of an Fe(Si) alloy, followed by its transformation into the stoichiometric Fe_3Si phase, and the growth of an Fe film. The critical Fe thickness necessary for that transformation was found to be 5 Fe monolayers.

Extensive work on the determination of the iron silicide constituents at the interfaces has been reported,[3–15] but the characterization of its dependence on the layer position in a multilayered stack has not been studied yet. This will be tackled in the present work on an $(Fe/Si)_3$ multilayer by ^{57}Fe conversion electron Mössbauer spectroscopy (CEMS), which allows studying Fe layers at selected depth. To this end we prepared a series of samples consisting of three sequentially deposited Fe/Si bilayers, where only one Fe layer consisted completely of highly enriched (95%) ^{57}Fe, while the other two were made of natural Fe, which contains ≃2.7% ^{57}Fe.

II. EXPERIMENTAL DETAILS

Multilayers with the full layer sequence GaAs/Fe(1 nm)/Ag(150 nm)/Fe(2.6 nm)/Si(1.5 nm)/Fe(2.6 nm)/Si(1.5 nm)/Fe(2.6 nm)/Si(10 nm) were prepared by thermal evaporation in a molecular-beam epitaxy system.[16] First, a buffer layer of Fe (1 nm)/Ag (150 nm) on a GaAs(001) substrate was prepared *in situ*, since this substrate has been reported to improve the crystalline quality of the Fe films and reduce roughness.[17] Then, three Fe layers with a nominal thickness of $d_{Fe} = 2.6$ nm separated by Si spacers of $d_{Si} = 1.5$ nm were deposited, where the last Si layer of 10 nm thickness serves as capping to avoid the oxidation of Fe. A series of three samples was prepared, each one containing only one out of the three Fe layers formed by ^{57}Fe. The samples will be

a)Electronic mail: lbadia@unizar.es

denoted C*i*, where $i = 1, 2, 3$ indicates the place of the ^{57}Fe layer in the multilayer stack. For instance, C1 makes reference to the sample with the first deposited Fe layer made of ^{57}Fe and the other two of natural Fe. An Fe foil of 95% enriched ^{57}Fe was used as target. The background pressure was better than 10^{-10} mbar. The thicknesses and the deposition rates, of about 0.6 nm/min for both Si and Fe (natural Fe and ^{57}Fe), were controlled by a calibrated quartz crystal monitor, and the layers were characterized by Auger electron spectroscopy and low-energy electron diffraction (LEED). All Fe and Si layers were deposited at RT. A well-defined LEED pattern observed throughout the Ag buffer and the first deposited Fe film indicated the starting point for a good epitaxial growth.[18]

High-resolution transmission electron microscopy (HRTEM) images were obtained in a FEI Titan Cube microscope operated at 300 kV and equipped with an image aberration corrector from CEOS. The HRTEM specimens were cross sectional lamellae of about 50 nm thickness fabricated in a FEI Helios 600 Nanolab. The single crystal substrate zone axis of the lamella was used to orient it to insure that the interfaces were perpendicular to the image plane; i.e., parallel to the direction of the electron beam.

The CEMS spectra were acquired at room temperature using a constant acceleration spectrometer with symmetrical waveform and a ^{57}Co (25 mCi) in Rh matrix source. A Rikon-5 detector with a 96%He-4%N_2 mixture gas was used.

III. RESULTS AND DISCUSSION

A. Morphology study by HRTEM

HRTEM images were collected on the as-deposited C1 sample to characterize the morphology of the films and interfaces. Fig. 1 shows a good epitaxial growth of the first Fe layer on the crystalline Ag(001) buffer, with thickness close to the nominal value and a sharp interface. In the alternation of layers of the subsequent deposition of Si and Fe the crystallinity of the second deposited Fe layer is still observed, while that of the third layer is hardly visible, both with increased interface roughness. In contrast, no crystal planes of the Si layers are observed, which indicates that the Si spacers have grown in an amorphous way, and therefore, the second and third deposited Fe layers have grown on amorphous Si spacers.

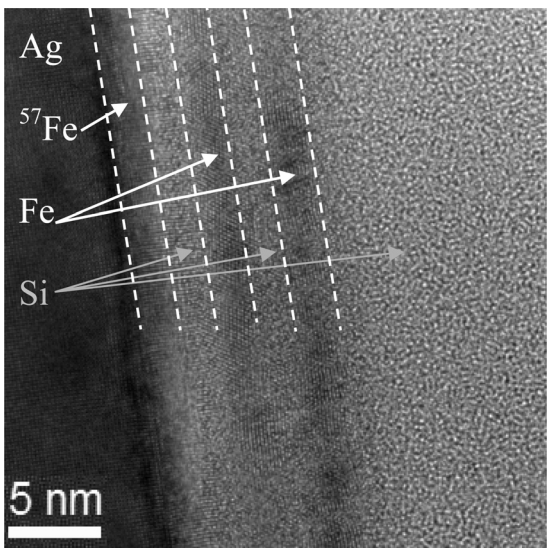

FIG. 1. HRTEM image of the C1 pristine sample.

B. Compositional study by CEMS

CEMS is a powerful tool to investigate the presence of Fe compounds in monolayers[19–22] and in multilayered systems.[2,11,15,23] This spectroscopy is a local probe for ^{57}Fe nuclei. The RT CEMS spectra from the present samples are depicted in Fig. 2. The spectrum of the first deposited Fe layer (sample C1) is clearly different from those of the subsequently deposited Fe layers (samples C2 and C3), which reflects that this ^{57}Fe layer was deposited directly on the crystalline Ag buffer, while in the other two samples the ^{57}Fe layers were grown on amorphous Si spacers.

Although the Mössbauer spectra of $Fe_{1-x}Si_x$ bulk alloys for concentrations up to almost $x = 0.27$ have been very well described in terms of a set of sextets related to Fe environments,[24–26] more recent works on Fe-Si multilayers[2,11,15] have used a nearly continuous distribution of sextets to account for the spectral intensity attributed to a ferromagnetic $Fe_{1-x}Si_x$ alloy. In the case of nanometric thin films the ratio of surface to volume number of Fe atoms is large. Therefore, the contribution of the interfacial Fe to the CEMS spectra is significant.

In the present work, we have chosen to fit the spectral intensity attributed to the $Fe_{1-x}Si_x$ alloy and the possible presence of α-Fe with a combination of several sextets in

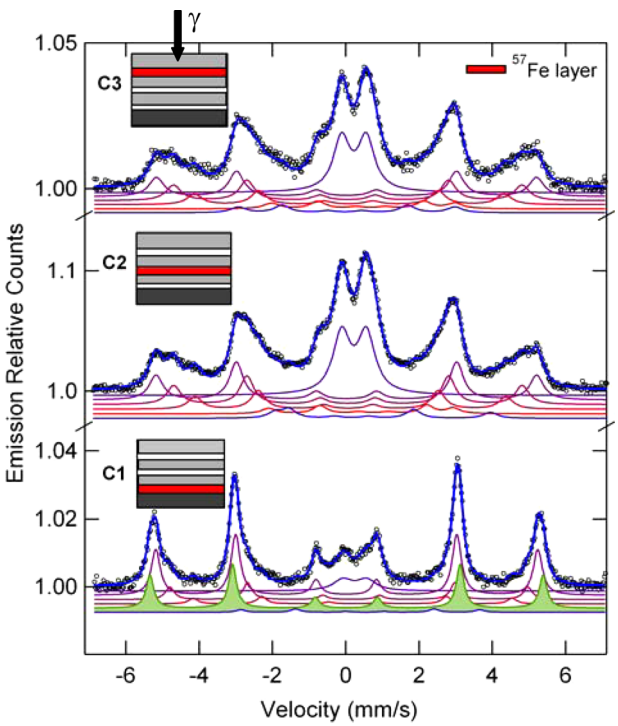

FIG. 2. RT CEMS spectra of the as-deposited C*i* ($i = 1, 2, 3$) samples, where *i* indicates the ^{57}Fe layer position in the multilayer deposition sequence. The α-Fe sextet on the bottom spectrum is shown as filled area (green). Inset: schematic representation of the multilayer, red indicates the ^{57}Fe layer position.

order to get deeper insight into the silicide phases distribution and to estimate the Si atomic concentration in the $Fe_{1-x}Si_x$ alloy.

To our knowledge this is the first assignment of Mössbauer components to specific Fe site environments in multilayer interfaces, with nanometric thin Fe layers. The experimental spectra were modelled including a doublet and the minimum number of sextets, which produced good fits with sensible hyperfine parameters. In particular, the criterium that an increasing isomer shift correlates with a decreasing hyperfine field is fulfilled, since it reflects the decreasing electronic charge density as the number of nearest neighbour (n.n.) Si atoms increases.[24] Hyperfine parameters and relative intensities are collected in Table I. Additionally, refinements with a doublet and a sextet distribution, as used in previous reports,[11,15] were performed to check that the set of fitted sextets accounted for all alloy contributions. In fact, both type of fits, i.e., with the set of sextets or the sextet distribution with hyperfine fields from 15 to 34 T, produced the same proportion of doublet area in the spectra.

The presence of several components in the CEMS spectra shows that during the deposition process, the ^{57}Fe atoms have diffused and reacted with the Si spacer, giving rise to the formation of intermediate silicide phases. According to previous works on the Fe-Si interfaces,[3,5,11,12,15,27–31] these compounds would have a magnetic $Fe_{1-x}Si_x$ alloy, and a paramagnetic silicide. The non-stoichiometric c-$Fe_{1-x}Si$ phase ($0 \leq x \leq 0.5$) has been proposed as that paramagnetic compound.[11,27,29,30,32–35]

We focus our attention on the analysis of the paramagnetic component given by the doublets. The c-FeSi phase with the cubic CsCl structure should show a singlet. However, Fe defective non-stoichiometric $Fe_{1-x}Si$, or strain at the interface, give rise to a distribution of locally non-cubic site symmetry, which is reflected in CEMS spectra as a doublet of large linewidth.[11,29]

In the present spectra, the fitted doublets show quadrupolar splittings ranging from $QS = 0.65(2)$ to $0.67(1)$ mm/s, isomer shifts from $\delta = 0.223(3)$ to $0.25(1)$ mm/s (with respect to α-Fe) and large linewidths $LW = 0.55(1)$ to $0.62(3)$ mm/s. This is consistent with the defective/strained paramagnetic c-$Fe_{1-x}Si$ phase.

Assuming identical recoilless fraction for every Fe site, the amount of the different Fe phases and, in particular, the occupation probability of ^{57}Fe atoms at various sites in an $Fe_{1-x}Si_x$ alloy can be obtained from the relative intensities of the spectral components. Specifically, the relative intensity (I) of the doublet yields the amount of the c-$Fe_{1-x}Si$ compound, which within the experimental errors is the same in the middle and top layers ($I = 0.33(2)$ and $0.30(3)$, respectively), and one half in the bottom layer ($I = 0.16(1)$) (see Table I). Therefore, the experiment on sample C1, which probes the bottom layer, allows us to identify the c-$Fe_{1-x}Si$ phase content of the Si on Fe interface. On the other hand, the spectra of samples C2 and C3 probe the middle and top layers, respectively. Since these layers contain both an Fe on Si and a Si on Fe interface, we can conclude by comparison with the doublet area in the C1 spectrum that the Si on Fe interface contains the same amount of c-$Fe_{1-x}Si$ as in the Fe on Si interface; i.e., the interfaces are symmetric regarding the paramagnetic c-$Fe_{1-x}Si$ phase. The relative intensity of the paramagnetic doublet can be correlated to the reduction of magnetization upon deposition of the nominal Fe layer thickness. It amounts to a reduction of the effective Fe layer thickness $\Delta d_{Fe} = 0.42$ nm *per* Fe/Si interface, over a total nominal value $d_{Fe} = 2.6$ nm. This is in agreement with previously reported values on Fe-Si multilayers.[11,32–34,36,37]

The analysis of the remaining sextet components is not straightforward and requires a comparison with the possible structures of the $Fe_{1-x}Si_x$ alloys. These have been long time ago studied in bulk samples[24,38–40] and in homogenous thin films prepared by co-deposition.[19–22] For x up to ~0.12 Si randomly substitutes Fe in the bcc structure of α–Fe, forming a disordered alloy. A transition from the disordered phase to an ordered one has been claimed to take place in a concentration range from 10% to 13% at. Si.[24,38–40] At $x = 0.25$, the stoichiometric compound Fe_3Si is formed (Fig. 3) with the $D0_3$ type structure; this is an ordered structure, where Si substitutes Fe only at the D sites under the steric constraint of a minimum Si-Si distance $\sqrt{2}a$ (be a the Fe-Fe interatomic distance).[24] Besides, Häggström *et al.*[25] have concluded that for concentrations between 8.6% and 23% at. Si, no homogeneous phase exists; instead, two phases, one disordered and the other with

TABLE I. Fitted hyperfine parameters obtained from the Ci ($i = 1, 2, 3$) CEMS spectra. I refers to the relative intensity of each component with respect to the total area of the spectrum, and I_s indicates the relative intensity with respect to the sum of sextet areas assigned to non-surface Fe atoms in $Fe_{1-x}Si_x$. The linewidth (LW) parameters of the sextets are correlated for each sample: $LW = 0.30(1)$, $0.45(1)$, and $0.49(1)$ mm/S for samples C1, C2, and C3, respectively. For the doublets, $LW = 0.62(3)$, $0.57(1)$, and $0.55(1)$ mm/s for sample Ci ($i = 1, 2, 3$), respectively.

	C1				C2				C3			
	QS (mm/s)	δ (mm/s)	I		QS (mm/s)	δ (mm/s)	I		QS (mm/s)	δ (mm/s)	I	
Doublet	0.65(2)	0.25(1)	0.16(1)		0.672 (3)	0.225(2)	0.33(2)		0.67(1)	0.223(3)	0.30(3)	
	B_{hf} (T)	δ (mm/s)	I	I_s	B_{hf} (T)	δ (mm/s)	I	I_s	B_{hf} (T)	δ (mm/s)	I	I_s
Sextet	33.28(6)	0.005(5)	0.23(4)	…	…	…	…	…	…	…	…	…
Sextet 1	32.33(5)	0.014(4)	0.42(4)	0.69(5)	32.20(3)	0.019(3)	0.25(1)	0.40(2)	32.15(6)	0.02(1)	0.24(3)	0.38(4)
Sextet 2	30.30(6)	0.116(7)	0.12(1)	0.19(2)	29.48(4)	0.057(3)	0.19(1)	0.31(2)	29.48(9)	0.052(7)	0.19(2)	0.30(4)
Sextet 3	26.98(11)	0.211(14)	0.052(5)	0.09(1)	26.32(6)	0.100(5)	0.12(1)	0.19(2)	26.21(11)	0.08(1)	0.13(2)	0.21(4)
Sextet 4	20.2(3)	0.46(3)	0.023(4)	0.038(5)	18.21(11)	0.58(1)	0.06(1)	0.10(1)	18.34(20)	0.11(5)	0.07(2)	0.11(2)
Sextet 5	…	…	…	…	15.62(12)	0.588(2)	0.06(1)	…	15.53(20)	0.56(3)	0.07(1)	…

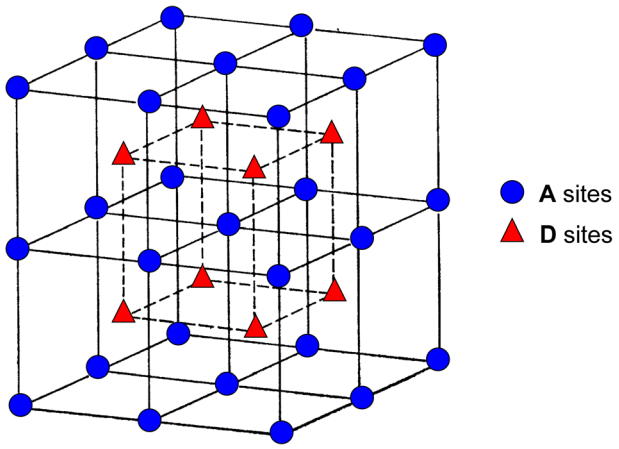

FIG. 3. Unit cell of an FeSi alloy structure. In Fe_3Si, the Fe atoms on D sites have 8 Fe-atoms as nearest neighbours, while Fe atoms on A sites have 4 Si atoms and 4 Fe atoms as nearest neighbours.

the DO_3 ordered structure would coexist. In contrast to bulk, sputtered $Fe_{1-x}Si_x$ silicide thin films have been reported to be amorphous for concentrations above 20% at. Si.[41]

The Fe site occupation probability in the disordered phase is described by a binomial distribution $P(n, m, \xi)$, where an Fe atom can be surrounded by m substituting Si atoms up to $n = 8$, the total number of n.n. sites in the bcc structure,[24] and

$$P(n, m, \xi) = \frac{n!}{m!(n-m)!}\xi^m(1-\xi)^{n-m}, \qquad (1)$$

with $\xi = x$. In contrast, in the ordered structure, Si atoms are assumed to enter only D sites and will be surrounded by 8 Fe atoms at A sites, while each Fe atom at an A site can have a variable number of n.n. Si atoms at D sites (Fig. 3). For a Si concentration x, the occupancy of Fe at D sites is $p_D = 1 - 0.5/(1-x)$, while that of an Fe atom at an A site surrounded by k Fe atoms placed at the n.n. D sites (environment Ak) is $p_{Ak} = (1-p_D)P(8, 8-k, \xi)$ with $\xi = 2x$ if no steric constraint between Si atoms is applied, or $P_{Ak} = (1-p_D)$ $P(4, 4-k, \xi)$ with $\xi = 4x$ if Si atoms are constrained to be separated a distance $\sqrt{2}a$. Such a constraint can be fulfilled for up to $x = 0.25$, i.e., the Fe_3Si alloy. More complex atomic substitution schemes have been proposed, where Si atoms are allowed to use both A and D sites, and the next n.n. effects are taken into account.[25,26]

1. Bottom ^{57}Fe layer

The CEMS spectrum of sample C1 provides information about the bottom layer in the $(Fe/Si)_3$ multilayered structure. In contrast to the middle and top Fe layers, it was deposited on the Ag buffer and it has only one Fe/Si interface; then Fe silicides can be formed only from one side. All sextets have been fitted with a common linewidth ($LW = 0.30(1)$ mm/s), which is similar to those reported on bulk $Fe_{1-x}Si_x$ alloys.[25,26] Five sextets with hyperfine fields from 33.3 to 20.2 T are found in the spectrum (Table I). The sextet with the highest hyperfine field ($B_{hf} = 33.3$ T) is consistent with either α–Fe or a silicide in the disordered phase of low Si concentration. However, in the silicide hypothesis that sextet should have the highest relative intensity according to the probability distribution of Fe n.n. environments (Table II), and a very low contribution of sextets with B_{hf} below 27 T.[24] This is in contradiction with the observed value in Table I (C1, column I). Therefore, that sextet will be assigned to α–Fe deposited on the Ag buffer and the remaining four sextets to a silicide in the ordered phase.

The sextet with $B_{hf} = 32.33$ T corresponds to Fe atoms with all Fe n.n. and is indicative of a silicide in the ordered phase, where the reduction of the hyperfine field with respect to that of α–Fe is produced by second and third Fe n.n.[24,42] However, its relative intensity of 0.69 in the four sextets set is too high for such a phase, and points to a disordered silicide.

The reduction in the hyperfine field of the subsequent sextets, $B_{hf} = 30.30(6)$ T, 26.98(11) T, and 20.23(6) T reflects the increasing number of n.n. substitution. The assignment of these sextets to specific Fe environment should be based on the field reduction and the environment probabilities. However, the spectral contribution from Fe atoms at low probability environments is difficult to resolve as separated sextets and is included in that of high probability environments with a close number of n.n. The Mössbauer sextets have been previously assigned to several environment probability groupings.[24–26] Since for $x > 0.15$, the A8 and A7 environments have much lower probabilities than those of D and A6 (Table II), the aforementioned field sequence can be assigned to A6, A5, and A4 environments, while A8 and A7 can be added to the spectral intensity of environment D, as in Ref. 24. However, no agreement between experimental sextet areas and environment probabilities is found for any particular Si concentration neither in the disordered nor ordered phase.

As suggested by Häggström *et al.*,[25] a two phase system could have been produced in this Fe layer between the c-$Fe_{1-x}Si$ layer and α–Fe, one with $x < 0.1$ (disordered phase, where Fe environments with more than 3 substituted n.n. atoms have very low probability), and another with $x > 0.15$ (ordered phase with highest probabilities of D sites and 3 or more substituted n.n. atoms). We propose that in this layer, there are three sublayers, the α–Fe, the c-$Fe_{1-x}Si$

TABLE II. Calculated probabilities of different Fe site occupancy and environments for $Fe_{1-x}Si_x$ alloys of selected Si atomic concentrations.

	Number of n.n. Fe atoms						
x	8	7	6	5			
0.04	0.721	0.240	0.035	0.003			
0.05	0.663	0.279	0.051	0.005			
	Type of site						
	D	A8	A7	A6	A5	A4	A3
0.15	0.412	0.015	0.090	0.203	0.203	0.076	…
0.16	0.405	0.010	0.071	0.190	0.225	0.100	…
0.18	0.390	0.004	0.039	0.149	0.255	0.164	…
0.25	0.333	…	…	…	…	0.667	…
0.26	0.324	…	…	…	…	0.574	0.096

and in between, the Fe-Si alloyed layer composed of an ordered and a disordered silicide phase.

2. Middle and top ^{57}Fe layers

The spectra of samples C2 and C3 are produced by the middle and top Fe layers, respectively. A set of up to five sextets were included in the fit. In contrast to the bottom layer, there is no sextet with $B_{hf} \simeq 33$ T, which is consistent with the presence of $Fe_{1-x}Si_x$ alloys in the ordered phase with high Si concentration and no α-Fe. The sequence of hyperfine fields is similar to that of the bottom layer, but the distribution of relative areas is completely different. Moreover, a low hyperfine field sextet of $B_{hf} = 15.6$ T contributes to both spectra, which should be related to Fe atoms surrounded by more than four n.n. Si atoms, as previously observed in bulk alloys.[24–26] This sextet was found in alloys with $x \geq 0.25$, where only two other sextets were present at ≃31 and ≃20–22 T. In the present case of layers of 2.6 nm thickness, fitting the spectra requires four sextets with hyperfine fields in the range 32 to 18 T, which discards a silicide with $x \geq 0.25$. Therefore, the sextet with $B_{hf} = 15.6$ T will be assigned to Fe atoms at the interface between the c-$Fe_{1-x}Si$ phase and the $Fe_{1-x}Si_x$ alloy layer. Indeed, the Fe atoms at this interface have a larger number of Si n.n. than within the $Fe_{1-x}Si_x$ bulk.

The remaining four sextets can now be assigned to an $Fe_{1-x}Si_x$ phase with Fe atoms in environments similar to those in the bulk alloys. The full sextet-environment assignment requires that all possible environments are resolved as spectral components. The calculated environment probabilities can be grouped to relate fitted sextets to corresponding Fe environments.[24] Within the experimental spectrum statistics and considering that, (a) for a given Si concentration, x, certain environments have low probability, (b) the hyperfine fields depend on both the number of n.n. and next n.n. Si atoms, we put forward the following interpretation: The four sextets of the spectra of the middle and top Fe layers can be assigned to an alloy with a concentration $x \simeq 0.15$ with the following site environment groupings: D + A8, A7 + A6, A5, and A4. The D + A8 grouping corresponds to environments with all Fe atoms as n.n., whose only difference stems from next n.n., but the D site probability dominates by a factor ≃30 (Table II). The sextet from Fe atoms with the low probability A7 environment is not resolved and its intensity is accounted for by the large A6 sextet. Both A6 and A5 sextets have similar and high intensities and can be clearly resolved. Finally, the low intensity A4 sextet is also resolved since its hyperfine field is well separated from the others.

The phases and their relative amounts in each Fe layer are collected in Table III. The saturation magnetization of the full multilayer can be estimated from that distribution. Since c-$Fe_{1-x}Si$ is paramagnetic and considering: (a) that the average Si concentration for the inhomogeneous Fe-Si alloy at the bottom layer is the same than that of the other two layers ($x = 0.15$), and (b) the saturation magnetization values are 1740 emu/cm^3 and 1230 emu/cm^3 for α-Fe and $Fe_{0.85}Si_{0.15}$,[43] respectively, one obtains an estimated magnetization $M_s = 7.37 \times 10^{-4}$ emu/cm^2 at RT. The experimental magnetization measured at RT with a SQUID magnetometer, after subtracting the magnetic contribution of the 1 nm Fe buffer layer, is 6.84×10^{-4} emu/cm^2. The estimated magnetization is only 8% above the experimental value, which strongly supports the phase distribution derived from the CEMS spectra.

TABLE III. Proportion, in %, of the different silicide phases present in each C*i* sample. In samples C2 and C3, the proportion includes Fe atoms at the FeSi to $Fe_{1-x}Si_x$ interface.

Silicide phase	C1	C2	C3
c-$Fe_{1-x}Si$	16%	33%	30%
α-Fe	23%	…	…
$Fe_{1-x}Si_x$	61%	67%	70%
with x:	Two phases	≃ 0.15	≃ 0.15

IV. CONCLUSIONS

The morphology and phase distribution in GaAs/Fe(1 nm)/Ag(150 nm)/Fe(2.6 nm)/Si(1.5 nm)/Fe(2.6 nm)/Si(1.5 nm)/Fe(2.6 nm)/ Si(10 nm) multilayers have been studied by HRTEM and CEMS. The HRTEM images show that the Si spacers grow in an amorphous way, while the first deposited Fe layer (bottom layer) shows a good epitaxial growth on the crystalline Ag buffer. In contrast, the middle and top Fe layers crystallize on amorphous Si spacers.

The CEMS spectrum of each Fe layer has been analysed using a discrete set of sextets, instead of a quasi-continuous distribution of sextets previously used in similar samples,[11,15] and a doublet. The fitted intensities and hyperfine fields have been related to the occupation and next neighbour environments of crystallographic sites of Fe atoms.

The contribution to the CEMS spectra of one of the Si/Fe interfaces (that on top of the first deposited Fe layer) is identified, and singled out from the contributions due to the Fe/Si interfaces. Having achieved this goal, it can be compared to the CEMS spectra of the other two Fe layers, for which both Si/Fe and Fe/Si interfaces are measured simultaneously. We conclude that the paramagnetic contribution is similar in both types of interfaces, Si/Fe and Fe/Si. This paramagnetic part contains 16% of the nominal Fe deposited in the Fe layer, *per* interface. It is assigned to the defective/strained c-$Fe_{1-x}Si$ phase.

The spectrum of the bottom layer has revealed the presence of the α-Fe phase in contact with the crystalline Ag buffer, and an $Fe_{1-x}Si_x$ layer of inhomogeneous concentration. In contrast, no α-Fe is present in the middle and top Fe layers. These spectra show the existence of an $Fe_{1-x}Si_x$ phase with a Si concentration $x \simeq 0.15$, and an additional contribution of Fe atoms at the interface between this phase and the adjacent paramagnetic phase.

Moreover, it has been found that the composition of nominal nanometric thin Fe layers (≃2–3 nm) depends on its position in the multilayer. The first Fe layer deposited on crystalline Ag in this case allows for good epitaxial growth and α-Fe remains, while in the upper layers, Fe is completely alloyed to form $Fe_{1-x}Si_x$ silicides.

ACKNOWLEDGMENTS

The financial support of the Spanish MINECO MAT2011-23791, the Aragonese DGA-IMANA E34 (co-funded by Fondo Social Europeo) and that received from the European Union FEDER funds is acknowledged. L.B.-R. acknowledges the Spanish MINECO FPU 2010 grant.

[1]R. R. Gareev, D. E. Bürgler, M. Buchmeier, D. Olligs, R. Schreiber, and P. Grünberg, Phys. Rev. Lett. **87**, 157202 (2001).
[2]G. J. Strijkers, J. T. Kohlhepp, H. J. M. Swagten, and W. J. M. de Jonge, Phys. Rev. Lett. **84**, 1812 (2000).
[3]M. Gomoyunova, D. Malygin, I. Pronin, A. Voronchikhin, D. Vyalikh, and S. Molodtsov, Surf. Sci. **601**, 5069 (2007).
[4]J. M. Gallego, J. M. García, J. Alvarez, and R. Miranda, Phys. Rev. B **46**, 13339 (1992).
[5]R. Kläsges, C. Carbone, W. Eberhardt, C. Pampuch, O. Rader, T. Kachel, and W. Gudat, Phys. Rev. B **56**, 10801 (1997).
[6]Q. Zhu, H. Iwasaki, E. D. Williams, and R. L. Park, J. Appl. Phys. **60**, 2629 (1986).
[7]B. Li, M. Ji, J. Wu, and C. Hsu, J. Appl. Phys. **68**, 1099 (1990).
[8]M. De Crescenzi, G. Gaggiotti, N. Motta, F. Patella, A. Balzarotti, and J. Derrien, Phys. Rev. B **42**, 5871 (1990).
[9]J. M. Gallego and R. Miranda, J. Appl. Phys. **69**, 1377 (1991).
[10]G. Crecelius, Appl. Surf. Sci. **65**, 683 (1993).
[11]G. J. Strijkers, J. T. Kohlhepp, H. J. M. Swagten, and W. J. M. de Jonge, Phys. Rev. B **60**, 9583 (1999).
[12]S. R. Naik, S. Rai, G. S. Lodha, and R. Brajpuriya, J. Appl. Phys. **100**, 013514 (2006).
[13]S. R. Naik, S. Rai, M. K. Tiwari, and G. S. Lodha, J. Phys. D: Appl. Phys. **41**, 115307 (2008).
[14]E. Chubunova, I. Khabelashvili, Y. Lebedinskii, V. Nevolin, and A. Zenkevich, Thin Solid Films **247**, 39 (1994).
[15]A. Gupta, D. Kumar, and V. Phatak, Phys. Rev. B **81**, 155402 (2010).
[16]R. R. Gareev, D. E. Bürgler, M. Buchmeier, R. Schreiber, and P. Grünberg, J. Magn. Magn. Mater. **240**, 235 (2002).
[17]D. Bürgler, C. Schmidt, J. Wolf, T. Schaub, and H.-J. Guntherodt, Surf. Sci. **366**, 295 (1996).
[18]M. Buchmeier, B. K. Kuanr, R. R. Gareev, D. E. Bürgler, and P. Grünberg, Phys. Rev. B **67**, 184404 (2003).
[19]M. Fanciulli, G. Weyer, H. Känel, and N. Onda, Phys. Scr. **T54**, 16 (1994).
[20]M. Fanciulli, C. Rosenblad, G. Weyer, H. V. Känel, N. Onda, V. Nevolin, and A. Zenkevich, MRS Proc. **402**, 319 (1995).
[21]M. Fanciulli, G. Weyer, A. Svane, N. E. Christensen, H. Von Känel, E. Müller, N. Onda, L. Miglio, F. Tavazza, and M. Celino, Phys. Rev. B **59**, 3675 (1999).
[22]M. Walterfang, W. Keune, K. Trounov, R. Peters, U. Rücker, and K. Westerholt, Phys. Rev. B **73**, 214423 (2006).
[23]S. N. Varnakov, S. G. Ovchinnikov, J. Bartolomé, J. Rubín, L. Badía, and G. V. Bondarenko, Solid State Phenom. **168**, 277 (2011).
[24]M. B. Stearns, Phys. Rev. **129**, 1136 (1963).
[25]L. Häggström, L. Granas, R. Wappling, and S. Devanarayanan, Phys. Scr. **7**, 125 (1973).
[26]G. Rixecker, P. Schaaf, and U. Gonser, Phys. Status Solidi A **139**, 309 (1993).
[27]L. T. Vinh, J. Chevrier, and J. Derrien, Phys. Rev. B **46**, 15946 (1992).
[28]E. E. Fullerton, J. E. Mattson, S. R. Lee, C. H. Sowers, Y. Y. Huang, G. Felcher, S. D. Bader, and F. T. Parker, J. Appl. Phys. **73**, 6335 (1993).
[29]S. Degroote, M. H. Langelaar, T. Kobayashi, J. Dekoster, J. D. Watchter, R. Moons, L. Niesen, and G. Langouche, Mater. Res. Soc. Symp. Proc. **320**, 133 (1993).
[30]J. E. Mattson, E. E. Fullerton, S. Kumar, S. R. Lee, C. H. Sowers, M. Grimsditch, S. D. Bader, and F. T. Parker, J. Appl. Phys. **75**, 6169 (1994).
[31]R. Brajpuriya, R. K. Sharma, A. Vij, and T. Shripathi, J. Mod. Phys. **2**, 864 (2011).
[32]A. Chaiken, R. P. Michel, and M. A. Wall, Phys. Rev. B **53**, 5518 (1996).
[33]J. J. de Vries, J. Kohlhepp, F. J. A. den Broeder, R. Coehoorn, R. Jungblut, A. Reinders, and W. J. M. de Jonge, Phys. Rev. Lett. **78**, 3023 (1997).
[34]J. de Vries, J. Kohlhepp, F. den Broeder, P. Verhaegh, R. Jungblut, A. Reinders, and W. de Jonge, J. Magn. Magn. Mater. **165**, 435 (1997).
[35]S. Amir, M. Gupta, A. Gupta, K. Ambika, and J. Stahn, Appl. Surf. Sci. **277**, 182 (2013).
[36]L. Badía-Romano, J. Rubín, C. Magén, F. Bartolomé, J. Sesé, M. R. Ibarra, J. Bartolomé, A. Hierro-Rodríguez, J. I. Martín, J. M. Alameda, D. E. Bürgler, S. N. Varnakov, S. V. Komogortsev, and S. G. Ovchinnikov, J. Magn. Magn. Mater. **364**, 24 (2014).
[37]S. N. Varnakov, J. Bartolomé, J. Sesé, S. G. Ovchinnikov, S. V. Komogortsev, A. S. Parshin, and G. V. Bondarenko, Phys. Solid State **49**, 1470 (2007).
[38]G. Phragmin, J. Iron Steel Inst., London **116**, 397 (1926).
[39]F. W. Glaser and W. Ivanick, Trans. Am. Inst. Min. Metall. Pet. Eng. **206**, 1290 (1956).
[40]M. C. Farquhar, H. Lipson, and A. R. Weill, J. Iron Steel Inst., London **152**, 457 (1945).
[41]Y. Shimada and H. Kojima, J. Appl. Phys. **47**, 4156 (1976).
[42]T. Cranshaw, C. Johnson, M. Ridout, and G. Murray, Phys. Lett. **21**, 481 (1966).
[43]L. K. Varga, F. Mazaleyrat, J. Kovac, and J. M. Greneche, J. Phys.: Condens. Matter **14**, 1985 (2002).